


Magneto-sensitivity in Dipolarly Coupled Three-Spin Systems

Robert H. Keens,^{*} Salil Bedkihal,^{*} and Daniel R. Kattnig[†]
*Living Systems Institute and Department of Physics, University of Exeter,
 Stocker Road, Exeter, Devon, EX4 4QD, United Kingdom*

 (Received 8 June 2018; published 27 August 2018)

The radical pair mechanism is a canonical model for the magneto-sensitivity of chemical reaction processes. The key ingredient of this model is the hyperfine interaction that induces a coherent mixing of singlet and triplet electron spin states in pairs of radicals, thereby facilitating magnetic field effects (MFEs) on reaction yields through spin-selective reaction channels. We show that the hyperfine interaction is not a categorical requirement to realize the sensitivity of radical reactions to weak magnetic fields. We propose that, in systems comprising three instead of two radicals, dipolar interactions provide an alternative pathway for MFEs. By considering the role of symmetries and energy level crossings, we present a model that demonstrates a directional sensitivity to fields weaker than the geomagnetic field and remarkable spikes in the reaction yield as a function of the magnetic field intensity; these effects can moreover be tuned by the exchange interaction. Our results further the current understanding of the effects of weak magnetic fields on chemical reactions, could pave the way to a clearer understanding of the mysteries of magnetoreception and other biological MFEs and motivate the design of quantum sensors. Further still, this phenomenon will affect spin systems used in quantum information processing in the solid state and may also be applicable to spintronics.

DOI: 10.1103/PhysRevLett.121.096001

There is growing excitement about the possibility of quantum coherence and entanglement underpinning the optimal functioning of biological processes [1]. A notable example is the avian inclination compass [2–12], which has recently been realized as a truly quantum-biological process [3]. The leading explanation of this phenomenon utilizes the radical pair mechanism (RPM), which describes the unitary evolution of singlet-triplet ($S - T$) coherences in systems comprising two radicals, i.e., two electron spins [2,13,14]. The RPM has also been suggested to underpin controversial health-related implications of exposure to weak electromagnetic fields [15–18]. For these phenomena, the so-called low-field effect (LFE) is crucial to foster sensitivity to magnetic fields of intensity comparable to the geomagnetic field ($\approx 50 \mu\text{T}$) [6,19–24]. The electron-electron dipolar interaction is often neglected when addressing MFEs within the RPM framework, but preliminary explorations have been conducted: electron-electron dipolar coupling is expected to resemble the exchange coupling, which, as the dominant interaction, suppresses $S - T$ conversion by lifting the near degeneracy of triplet and singlet states, reducing their susceptibility to mixing by weak hyperfine interactions [25], and quenching the LFE [26]. Efimova *et al.* proposed that the dipolar interaction could be partly compensated by the exchange interaction, thereby allowing high sensitivity to the geomagnetic field despite sizable electron-electron dipolar coupling interactions [27].

In contrast to the two-spin systems of the classical RPM, spin triads have attracted comparably little attention.

Systems of three spins have been discussed: in the context of spin catalysis [28], the chemical Zeno effect [24,29], quantum teleportation [30], and as a decoherence pathway [31]. In spin catalysis, the exchange coupling of the radical pair with the spin catalyst is the main interaction motif. As the Zeeman part of the Hamiltonian commutes with the exchange Hamiltonian, this interaction alone is insufficient to produce MFEs (see Supplemental Material [32]). However, mutual exchange coupling can provide the premise for near level crossings at certain strengths of an external magnetic field, whereupon hyperfine-driven spin conversion can proceed efficiently [36,37], and may also transmit the effect of a fast-relaxing third radical [38]. A perturbative approach based on a Hubbard-trimer Hamiltonian has been used to show that the additional radical can enhance the intersystem crossing rate [39]. Spin coherence transfer in the three-radical system has been recently realized experimentally [39]. Furthermore, the spin-selective reaction of a radical pair with a scavenger radical has been shown to boost anisotropic magnetic field effects [40] and provide resilience to spin relaxation in one of the radicals of the triad [24], thereby providing decisive advantages over the classical RPM model of magnetoreception. To our knowledge, three-spin systems have only been discussed in the biological context in Refs. [24,30,40]. All models mentioned in this context have disregarded the effects of electron-electron dipolar interactions.

We consider a toy model of three spins in an external magnetic field and investigate the MFEs that arise as a

consequence of interradical interaction. Our model Hamiltonian is given (in angular frequency units) by

$$\begin{aligned}\hat{H} &= \hat{H}_0 + \hat{H}_1 = \hat{H}_{\text{dd}} + \hat{H}_{\text{ex}} + \hat{H}_1 \\ &= \sum_{i<j}^N \hat{\mathbf{S}}_i \cdot \mathbf{D}_{i,j} \cdot \hat{\mathbf{S}}_j - \sum_{i<j}^N J_{i,j} \left(\frac{1}{2} + 2\hat{\mathbf{S}}_i \cdot \hat{\mathbf{S}}_j \right) \\ &\quad + \gamma \vec{\mathbf{B}}_0 \cdot \sum_i^N \hat{\mathbf{S}}_i.\end{aligned}\quad (1)$$

The individual summands account for the electron-electron dipolar (\hat{H}_{dd}), exchange (\hat{H}_{ex}), and Zeeman interactions (\hat{H}_1). $\vec{\mathbf{B}}_0$ denotes the applied magnetic field, B_0 its intensity, and $\gamma = [(g\mu_B)/\hbar]$. Here, we have assumed that the Zeeman interaction is isotropic and identical for all radicals on account of our focus on the MFEs of organic radicals in weak magnetic fields, i.e., $g \approx 2$ and the anisotropies are negligible for moderate B_0 . The electron-electron dipolar interactions are treated in the point-dipole limit. The interaction energy is related to the (supra)-molecular structure of the spin triad by

$$\hat{\mathbf{S}}_i \cdot \mathbf{D}_{i,j} \cdot \hat{\mathbf{S}}_j = d_{i,j}(r_{i,j})[\hat{\mathbf{S}}_i \cdot \hat{\mathbf{S}}_j - 3(\hat{\mathbf{S}}_i \cdot \vec{\mathbf{e}}_{i,j})(\hat{\mathbf{S}}_j \cdot \vec{\mathbf{e}}_{i,j})]. \quad (2)$$

In the above equation, $\vec{\mathbf{e}}_{i,j} = [(\vec{\mathbf{r}}_{i,j})/|\vec{\mathbf{r}}_{i,j}|]$, where $\vec{\mathbf{r}}_{i,j}$ is the vector connecting radical centers i and j , $d_{i,j} = (d_0/|\vec{\mathbf{r}}_{i,j}|^3)$, and $d_0 = [\mu_0/(4\pi\hbar)]g^2\mu_B^2$. We assume that the three-radical system is generated in the singlet state of radicals 1 and 2 with the third radical uncorrelated to the others; i.e., the initial density operator obeys $\hat{\rho}(t=0) = \frac{1}{2}\hat{P}_s^{(1,2)}$ where $\hat{P}_s^{(i,j)} = \frac{1}{4} - \hat{\mathbf{S}}_i \cdot \hat{\mathbf{S}}_j = \frac{1}{2}(1 - \hat{P}_{i,j})$ is the singlet projection operator on the i, j -subspace, and $\hat{P}_{i,j}$ is the permutation operator for spins i and j . Assuming that radicals 1 and 2 recombine with equal rate constant k in the singlet and triplet configurations, the equation of motion for the spin-triad density matrix becomes

$$\frac{d\hat{\rho}(t)}{dt} = -i[\hat{H}, \hat{\rho}(t)] - k\hat{\rho}(t). \quad (3)$$

The quantum yield of the singlet recombination product of radicals 1 and 2 is $\varphi_s = k \int_0^\infty d\tau \text{Tr}[\hat{P}_s^{(1,2)}\hat{\rho}(\tau)]$, and the powder-averaged singlet yield is $\langle \varphi_s \rangle = [1/(4\pi)] \int_0^{2\pi} d\phi \int_0^\pi d\vartheta \sin(\vartheta) \varphi_s[B_0(\vartheta, \phi)]$. The MFEs can then be quantified by $\chi_s = [\varphi_s(B_0)/\varphi_s(0)] - 1$; analogous definitions apply to the orientation-averaged yield. In the eigenbasis of the Hamiltonian, \hat{H} , we find that $\varphi_s = \frac{1}{2} \sum_{i,j} \langle i | \hat{P}_s^{(1,2)} | j \rangle^2 f(k, \omega_i - \omega_j)$, where $f(k, \Delta\omega) = [k^2/(k^2 + \Delta\omega^2)]$, and $|i\rangle, |j\rangle$ are the eigenstates of \hat{H} . We show in the Supplemental Material [32] that the conclusions we draw using this approach are still qualitatively

valid if recombination proceeds at different rates in the singlet and triplet configuration.

The magnetic field independent part of the Hamiltonian (\hat{H}_0) is invariant under time reversal symmetry; i.e., it commutes with the time reversal operator $\hat{\Theta} = e^{i\pi\hat{S}_y}\hat{K}$, where \hat{K} denotes complex conjugation in the standard basis, and \hat{S}_y is the y component of the total spin-angular momentum operator $\hat{\mathbf{S}} = \sum_j \hat{\mathbf{S}}_j$. As $\hat{\Theta}^2 = -1$, the eigenstates of \hat{H}_0 are (at least) twofold degenerate (Kramers degeneracy [41]). Furthermore, as $\hat{\Theta}$ maps $|S^{(1,2)\pm}\rangle$ into $\pm|S^{(1,2)\mp}\rangle$, pairwise degenerate states ($|i\rangle, \hat{\Theta}|i\rangle$) yield the same expectation value of $\hat{P}_s^{(1,2)}$. Note, however, that $|S^{(1,2)\pm}\rangle$ is not an eigenstate of the Hamiltonian, in stark contrast to the well-studied scenarios of pairs of radicals. This Kramers degeneracy, in spin triads, is broken by an external magnetic field. Consequently, the energy levels split and, depending on symmetry properties, can cross and/or anticross as a function of the applied field. This gives rise to prominent MFEs by impacting upon the coupling matrix elements $\langle i | \hat{P}_s^{(1,2)} | j \rangle$ and $f(k, \Delta\omega)$ (through altered energy differences). An example of such degeneracy lifting is shown schematically in Fig. 1(a). The necessary and sufficient conditions to observe MFEs are that (i) $[\hat{P}_s^{(1,2)}, \hat{H}_0] \neq 0$ and (ii) \hat{H}_0 does not possess the $SU(2)$ spin rotation symmetry; see Supplemental Material [32] for details. For a radical pair, \hat{H} always commutes with $\hat{P}_s^{(1,2)}$, and no MFEs are observed due to interradical

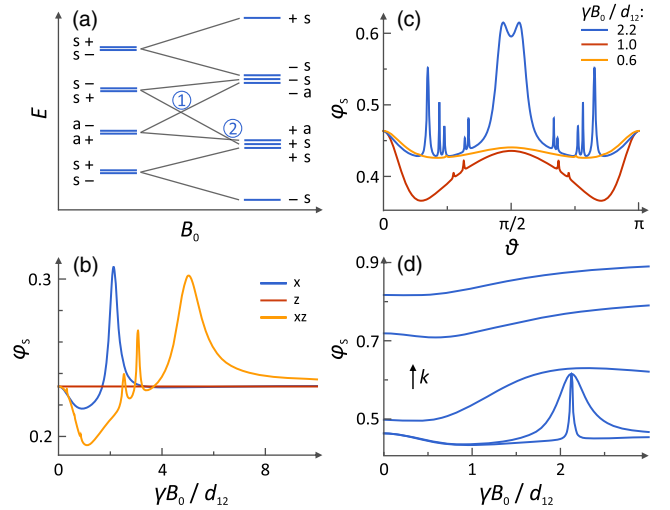


FIG. 1. (a) Schematic correlation diagram of energy level crossings as a function of the applied field B_0 . The labels classify the (anti-)symmetry of the states under $\hat{P}_{1,3}$ and \hat{X} . (b) Yield vs orientation for selected values of B_0 , here, the recombination constant $k/d_{1,2} = 0.01$. (c) Yield vs B_0 for selected orientations; here $k/d_{1,2} = 0.01$. (d) Yield vs B_0 for $k/d_{1,2} = 0.001, 0.01, 0.1, 0.5, 1$, respectively, and in ascending order. Here the Zeeman field is along the x direction. In all of the above figures, $J = 0$.

interactions. Here, we argue that dipolarly coupled spin triads give rise to MFEs for all configurations except for a peculiar one with the third (inert) radical placed halfway between the recombining radicals (and in the limit that radical 3 is so remote that it does not impact upon the spin evolution of the dyad on the timescale of its lifetime; see Supplemental Material [32]). On the contrary, a purely exchange-coupled isotropic spin system does not exhibit magnetosensitivity as a consequence of the retained $SU(2)$ symmetry of \hat{H}_0 , as shown in the Supplemental Material [32].

We first considered a linear symmetric triad for which $d_{1,2} = d_{2,3} = 8d_{1,3}$; the effect of changes to this geometry can be seen below and, in more detail, in the Supplemental Material [32]. For negligible exchange couplings ($J_{i,j} = 0$), Figs. 1(b)–1(d) show the singlet yield as a function of the magnetic field for selected orientations or as a function of orientation for selected fields. In the case where the magnetic field is parallel to the molecular symmetry axis, z , $[\hat{H}_{\text{dd}}, \hat{H}_1] = 0$; i.e., the z component of the total magnetization is conserved and no MFE arises. An analytic calculation reveals the dependence of the singlet yield on k [32]. In the limit of slow recombination, the yield approaches $[(841)/(1816)]$; for fast recombination no spin conversion is observed ($\varphi_S = 1$) as expected. For any other orientation of the magnetic field, the Zeeman Hamiltonian does not commute with the dipolar part and pronounced MFEs can be observed, as demonstrated in Fig. 1(b). With $B_0 \parallel x$, a marked spike is observed for $B_0 \approx 2.1d_{1,2}$. This peak is the consequence of the crossing of two energy levels, with different permutation symmetries but the same spin-inversion symmetry, as is schematically illustrated in the correlation diagram in Fig. 1(a). \hat{H} is symmetric with respect to the interchange of spins 1 and 3. Consequently, six of the eigenstates are symmetric and two are antisymmetric with respect to $\hat{P}_{1,3}$. For $B_0 \parallel x$, the latter two are proportional to $|\alpha\alpha\beta\rangle \pm |\alpha\beta\beta\rangle - |\beta\alpha\alpha\rangle \mp |\beta\beta\alpha\rangle$. The second of these (lower sign) crosses two of the states of the symmetric representation at $B_0 \approx 0.3812d_{1,2}$ and $B_0 = \frac{17}{8}d_{1,2}$. The spike results from the second of these crossings [labeled (2) in Fig. 1(a)]; for the first one, the matrix element of $\langle i|\hat{P}_s^{(1,2)}|j\rangle$ vanishes by symmetry. This is the case because, for $B_0 \parallel x$, $\hat{X} = \otimes_i \hat{\sigma}_{i,x}$, which exchanges α and β states, provides another symmetry element. Since $[\hat{X}, \hat{P}_s^{(1,2)}] = 0$, only crossings of the same \hat{X} symmetry can alter the MFE. As such, sharp changes in the reaction yield result from the level crossings between states of different symmetry provided that the off-diagonal matrix elements of the singlet projection operator do not vanish. For arbitrary magnetic field and orientation, the singlet yield has to be evaluated numerically. For high fields, all but the secular parts of \hat{H}_{dd} can be neglected and a perturbation-theoretical treatment yields an analytic expression of the singlet yield and its orientational dependence (given in the Supplemental

Material [32]). Its most obvious feature is the cessation of spin evolution for the magic angle.

For a disordered system, the observed singlet yield represents the average over all possible orientations of the external magnetic field vector \vec{B}_0 , with respect to the molecular axes of the system. Figure 2(a) shows this powder average of the singlet yield for the linear, symmetric spin triad over a range of k values. Interestingly, the recombination yield is not averaged to zero even though the average dipolar interaction of a pair of spins vanishes. The field dependence is characterized by a minimum at $B_0 \approx d_{1,2}$, which is the dominant feature at small k . We characterize the field effect by established measures such as the field of half-saturation $B_{1/2}$ [the field for which $\langle \varphi_S(B_0) \rangle$ equals $\frac{1}{2}(\langle \varphi_S(B=0) \rangle + \langle \varphi_S(B \rightarrow \infty) \rangle)$] and the MFEs associated with characteristic points such as the low-field minimum, which resembles the LFE documented for the hyperfine mechanism in radical pairs [19]. These parameters are summarized in Figs. 2(b) and 2(c) as a function of k . For B_0 exceeding a few $d_{1,2}$, huge field effects χ in excess of 30%, can be realized for intermediate k of the order of $0.2d_{1,2}$ [Fig. 2(c)]. The magnitude of the low-field feature is approximately 12% for small k values. For context, note that at a distance of 17 Å, $d_{1,2}$ will be of the order of 10 MHz and $k = 0.01d_{1,2}$ would then correspond to a lifetime of $k^{-1} = 1.6 \mu\text{s}$. Under these conditions, the low-field effect in dipolarly coupled spin triads is expected to closely agree with what the hyperfine mechanism can deliver for radical pairs (*vide infra* for a substantial enhancement). Note that significant MFEs can also ensue for comparably short coherence times

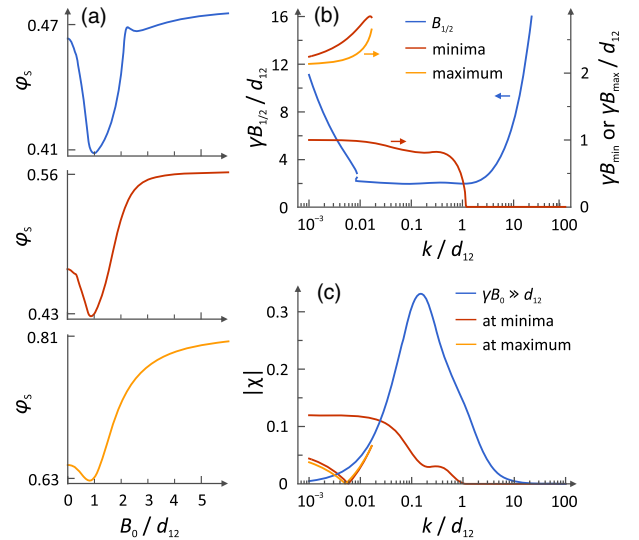


FIG. 2. (a) Powder averages for $k/d_{1,2} = 6.86 \times 10^{-3}$, 0.047, and 0.322, respectively. (b) MFE characterized by half saturation $B_{1/2}$, and the locations of minima (B_{\min}) and maxima (B_{\max}), as a function of $k/d_{1,2}$. (c) Absolute MFE vs $k/d_{1,2}$. In all of the above plots $J = 0$.

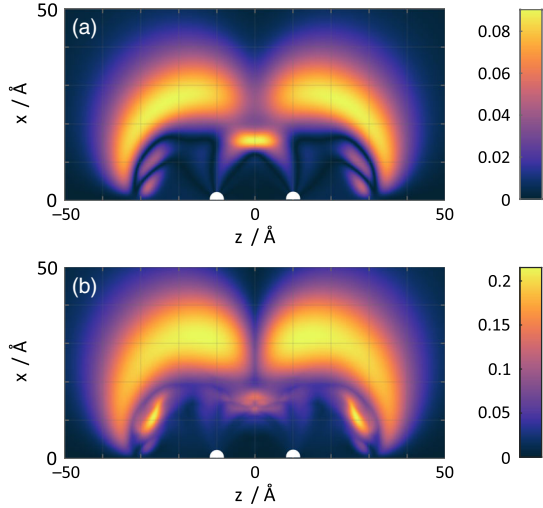


FIG. 3. (a) Absolute value of the MFE. (b) Anisotropy relative to the mean singlet yield. We use $k = 0.0245d_{1,2}$ and $B_0 = 0.215d_{1,2}$ corresponding to a lifetime of $1 \mu\text{s}$ and the geomagnetic field ($50 \mu\text{T}$) for an interradsical distance of 20 \AA , and $J = 0$. Spins 1 and 2 are located at $(0, a)$ and $(0, -a)$, respectively, with $a = 10 \text{ \AA}$, and the position of spin 3 is varied in the containing plane.

and, thus, quickly relaxing radicals could be meaningfully considered in the triad model for small r .

Substantial MFEs can, in fact, be observed for a variety of geometries of the spin triad. Figure 3 shows the dependence of the powder-averaged MFE and the relative anisotropy, i.e., the largest orientational spread of the singlet yield, relatively to the mean singlet yield, of general configurations for a magnetic field intensity of $50 \mu\text{T}$ (roughly the geomagnetic field). Assuming that spins 1 and 2 are located at $(0, a)$ and $(0, -a)$, respectively, with $a = 10 \text{ \AA}$, the maximum averaged MFE is $\approx 9\%$ at the location of the third spin ($\pm 1.58a, \pm a$). The maximum anisotropy amounts to 21.5% at $(\pm 3.18a, \pm 1.35a)$, which corresponds to interradsical distances as large as 40 \AA . Thus sizable MFEs are induced by the dipolar interaction even at relatively large distances, demonstrating that the effect does not rely on infrequent direct three-particle encounters, which could have a bearing on its relevance [24]. In the Supplemental Material [32] we show analogous results for $a = 7.5 \text{ \AA}$ and higher field intensities, with anisotropies in excess of 100% and MFEs far above 30% [32].

We further discuss the bond angle dependence for randomly oriented isosceles spin triads. For the geomagnetic field we observe the largest field effect for bond angles roughly corresponding to a pentagon's internal angle (144°) or slightly less than an equilateral triangle's (60°). For greater field intensities, large effects can be realized for all bond angles of practical relevance (see Supplemental Material [32]). Unlike for the linear geometry, we find that the MFEs of these systems typically do not decrease with increasing k^{-1} . For the equilateral triangular geometry,

sizable MFEs for k as large as $10d_{1,2}$ are predicted. These observations indicate that geometry indeed plays an important role, and that the MFEs in certain geometries may be less susceptible to variations in the lifetime. The system typically shows avoided crossings of energy levels, which nonetheless can give rise to spiky features [3,42].

We further studied the effect of an additional exchange interaction on the MFEs. As \hat{H}_{ex} displays time-reversal symmetry the eigenstates of the Hamiltonian are still double degenerate for $B_0 = 0$. Yet, remarkable LFEs can emerge if the (anti-)crossings of energy levels are shifted to lower magnetic fields. An illustrative example of this phenomenon is provided by the linear spin-triad for $J = J_{1,2} = J_{2,3}$ and $J_{1,3} = 0$, i.e., for the symmetric coupling of adjacent spins, and with the magnetic field perpendicular to the triad axis. As shown in Fig. 4(a), the singlet yield of this system exhibits a sharp peak, which shifts to lower magnetic field intensities for exchange couplings approaching $0.25 d_{1,2}$. Figure 4(c) then shows how the amplitude and field location of the peak vary as a function of the exchange coupling. It is interesting to note that, for typical dipolar coupling strengths, this feature may occur at field values smaller than the geomagnetic field. Formally, for these regions of maximal low-field sensitivity, the peak shifts from positive to negative magnetic field intensities. As shown in Figs. 4(c) and 4(d), the peak decreases in amplitude with increasing J and broadens as the recombination rate constant increases. It remains prominent for k up to $0.02d_{1,2}$ which, for typical parameters, equates to lifetimes of the order of microseconds (but could be less for

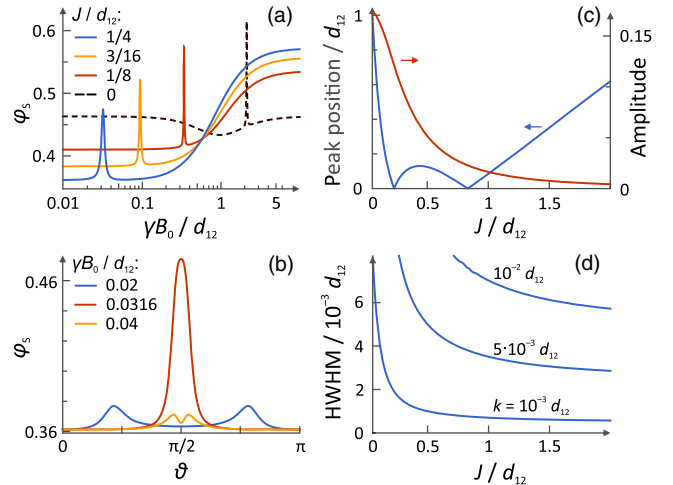


FIG. 4. (a) Yield vs applied field for different exchange interaction strengths, $J/d_{1,2}$; here, $k/d_{1,2} = 0.001$ and $B_0 \parallel x$. (b) Yield as a function of orientation for different B_0 ; we use $k/d_{1,2} = 0.001$. (c) The location and amplitude of a low-field peak's maximum, as a function of the exchange interaction strength with $k/d_{1,2} = 0.001$ and 0.01 (indistinguishable). (d) The half width at half maximum of a low-field peak as a function of $J/d_{1,2}$, for k as indicated in the figure.

smaller interrads distances). The Supplemental Material [32] summarizes the dependence of these characteristic parameters of the MFE as a function of k [32]. Importantly, the spike does appear in powder averages, suggesting that it could be relevant to MFEs in the randomly oriented samples implicated in biological radical reactions. Figure 4(b) shows how a large directional anisotropy can occur in the low-field regime. Here, J has been fixed to $\frac{1}{4}d_{1,2}$ and one can see that the spike results from an applied field $B_0 = 0.0316d_{1,2}$, while comparatively little directional anisotropy can be seen for other low-field intensities. For negative J , and $J > 2d_{1,2}$, the line shape does not exhibit a pronounced maximum; the main feature is a minimum at higher field. We have shown that remarkable MFEs can emerge in radical triads due to the dipolar interaction. This realization extends our current understanding of the magnetosensitivity of chemical reactions by providing an additional mechanistic pathway. Unlike the well-established RPM, this three-radical effect does not rely on hyperfine interactions or differing g factors. Because of the slow decay of the dipolar interaction with distance, aspects of this mechanism could be unexpectedly relevant, e.g., in the context of magnetoreception, the adverse health effects putatively associated with electromagnetic field exposure, or for purposefully engineered sensing applications, coherent control, quantum information processing with spins in the solid state and potentially spintronics [43–45]. In particular, the three-radical pathway could underlie the putative magnetosensitivity of lipid peroxidation, a process that follows a free-radical chain mechanism predominantly involving peroxy radicals derived from polyunsaturated fatty acids as chain carriers devoid of dominant hyperfine interactions [15–17,46]. In this context, it is remarkable that the effect can, in principle, provide MFEs of considerable amplitude and sensitivity to fields comparable to the geomagnetic field. For many radicals, the spin density is spread over several magnetic nuclei. In this case, $S - T$ transitions will be induced by the hyperfine interaction *and* the dipolar coupling among the radicals of the spin triad. It is surprising that this mechanism has so far remained unexplored.

We would like to thank The Royal Society (RG170378), the EPSRC (Grant No. EP/R021058/1) and NVIDIA (GPU Grant Program) for financial and in-kind support.

*R. H. K. and S. B. contributed equally to this work.

†D.R.Kattnig@exeter.ac.uk

- [1] N. Lambert, Y.-N. Chen, Y.-C. Cheng, C.-M. Li, G.-Y. Chen, and F. Nori, *Nat. Phys.* **9**, 10 (2013).
- [2] P. J. Hore and H. Mouritsen, *Annu. Rev. Biophys.* **45**, 299 (2016).
- [3] H. G. Hiscock, S. Worster, D. R. Kattnig, C. Steers, Y. Jin, D. E. Manolopoulos, H. Mouritsen, and P. J. Hore, *Proc. Natl. Acad. Sci. U.S.A.* **113**, 4634 (2016).
- [4] E. M. Gauger, E. Rieper, J. J. L. Morton, S. C. Benjamin, and V. Vedral, *Phys. Rev. Lett.* **106**, 040503 (2011).
- [5] J. Clausen, G. G. Guerreschi, M. Tiersch, and H. J. Briegel, *J. Chem. Phys.* **141**, 054107 (2014).
- [6] J. A. Pauls, Y. Zhang, G. P. Berman, and S. Kais, *Phys. Rev. E* **87**, 062704 (2013).
- [7] H. J. Hogben, T. Biskup, and P. J. Hore, *Phys. Rev. Lett.* **109**, 220501 (2012).
- [8] C. Y. Cai, Q. Ai, H. T. Quan, and C. P. Sun, *Phys. Rev. A* **85**, 022315 (2012).
- [9] T. Ritz, S. Adem, and K. Schulten, *Biophys. J.* **78**, 707 (2000).
- [10] M. Tiersch and H. J. Briegel, *Phil. Trans. R. Soc. A* **370**, 4517 (2012).
- [11] B.-M. Xu, J. Zou, J.-G. Li, and B. Shao, *Phys. Rev. E* **88**, 032703 (2013).
- [12] D. R. Kattnig, J. K. Sowa, I. A. Solov'yov, and P. J. Hore, *New J. Phys.* **18**, 063007 (2016).
- [13] C. T. Rodgers and P. J. Hore, *Proc. Natl. Acad. Sci. U.S.A.* **106**, 353 (2009).
- [14] U. E. Steiner and T. Ulrich, *Chem. Rev.* **89**, 51 (1989).
- [15] S. Ghodbane, A. Lahbib, M. Sakly, and H. Abdelmelek, *BioMed. Res. Intl.* **2013**, 602987 (2013).
- [16] U. Lalo, Y. Pankratov, and O. Mikhailik, *Redox Rep.* **1**, 71 (1994).
- [17] H. Kabuto, I. Yokoi, N. Ogawa, A. Mori, and R. P. Liburdy, *Pathophysiol. Haemost. Thromb.* **7**, 283 (2001).
- [18] J. Juutilainen, M. Herrala, J. Luukkonen, J. Naarala, and P. Hore, *Proc. R. Soc. B* **285**, 20180590 (2018).
- [19] C. Timmel, U. Till, B. Brocklehurst, K. Mclauchlan, and P. Hore, *Mol. Phys.* **95**, 71 (1998).
- [20] K. Maeda, K. B. Henbest, F. Cintolesi, I. Kuprov, C. T. Rodgers, P. A. Liddell, D. Gust, C. R. Timmel, and P. Hore, *Nature (London)* **453**, 387 (2008).
- [21] K. Maeda, A. J. Robinson, K. B. Henbest, H. J. Hogben, T. Biskup, M. Ahmad, E. Schleicher, S. Weber, C. R. Timmel, and P. Hore, *Proc. Natl. Acad. Sci. U.S.A.* **109**, 4774 (2012).
- [22] T. Suzuki, T. Miura, K. Maeda, and T. Arai, *J. Phys. Chem. A* **109**, 9911 (2005).
- [23] D. R. Kattnig, E. W. Evans, V. Déjean, C. A. Dodson, M. I. Wallace, S. R. Mackenzie, C. R. Timmel, and P. J. Hore, *Nat. Chem.* **8**, 384 (2016).
- [24] D. R. Kattnig, *J. Phys. Chem. B* **121**, 10215 (2017).
- [25] M. Zarea, R. Carmieli, M. A. Ratner, and M. R. Wasielewski, *J. Phys. Chem. A* **118**, 4249 (2014).
- [26] A. R. O'Dea, A. F. Curtis, N. J. B. Green, C. R. Timmel, and P. J. Hore, *J. Phys. Chem. A* **109**, 869 (2005).
- [27] O. Efimova and P. J. Hore, *Biophys. J.* **94**, 1565 (2008).
- [28] A. L. Buchachenko and V. L. Berdinsky, *J. Phys. Chem.* **100**, 18292 (1996).
- [29] A. S. Letuta and V. L. Berdinskii, *Dokl. Phys. Chem.* **463**, 179 (2015).
- [30] K. M. Salikhov, J. H. Golbeck, and D. Stehlik, *Appl. Magn. Reson.* **31**, 237 (2007).
- [31] V. I. Borovkov, I. S. Ivanishko, V. A. Bagryansky, and Y. N. Molin, *J. Phys. Chem. A* **117** (2013).
- [32] See Supplemental Material at <http://link.aps.org/supplemental/10.1103/PhysRevLett.121.096001> for explicit expressions for the dipolar coupling tensors used and mathematical justification of the symmetry arguments presented, which includes Refs. [33–35].

- [33] D. R. Kattnig, I. A. Solov'yov, and P. J. Hore, *Phys. Chem. Chem. Phys.* **18**, 12443 (2016).
- [34] R. Haberkorn, *Mol. Phys.* **32**, 1491 (1976).
- [35] A. T. Dellis and I. K. Kominis, *BioSystems* **107**, 153 (2012).
- [36] I. Magin, P. Purto, A. Kruppa, and T. Leshina, *Appl. Magn. Reson.* **26**, 155 (2004).
- [37] I. M. Magin, P. A. Purto, A. I. Kruppa, and T. V. Leshina, *J. Phys. Chem. A* **109**, 7396 (2005).
- [38] P. Hore, D. A. Hunter, F. G. van Wijk, T. J. Schaafsma, and A. J. Hoff, *BBA-Bioenergetics* **936**, 249 (1988).
- [39] S. Yeganeh, M. R. Wasielewski, and M. A. Ratner, *J. Am. Chem. Soc.* **131**, 2268 (2009).
- [40] D. R. Kattnig and P. Hore, *Sci. Rep.* **7**, 11640 (2017).
- [41] M. J. Klein, *Am. J. Phys.* **20**, 65 (1952).
- [42] D. V. Sosnovsky, G. Jeschke, J. Matysik, H.-M. Vieth, and K. L. Ivanov, *J. Chem. Phys.* **144**, 144202 (2016).
- [43] H. Liu, M. B. Plenio, and J. Cai, *Phys. Rev. Lett.* **118**, 200402 (2017).
- [44] V. R. Kortan, C. Şahin, and M. E. Flatté, *Phys. Rev. B* **93**, 220402 (2016).
- [45] A. Ghirri, A. Candini, and M. Affronte, *Magnetochemistry* **3**, 12 (2017).
- [46] D. A. Pratt, K. A. Tallman, and N. A. Porter, *Accounts Chem. Res.* **44**, 458 (2011).